Control-Oriented Modeling for Flexible Aircraft

Molong Duan*, Carlos E. S. Cesnik†, and Ilya V. Kolmanovsky‡
University of Michigan, Ann Arbor, MI, 48109, USA.

Fabio Vetrano§
Airbus Operations S.A.S., Toulouse, France.

Flexible aircraft designs with high aspect ratio wings and light-weight structures are increasingly adopted to achieve improved fuel efficiency. To design a controller for a flexible aircraft, a low-order model of its dynamics that captures the aeroelastic behavior is needed. One approach to establishing such a low-order model is to extend the 6-degree-of-freedom rigid aircraft model with additional elastic states. However, most of the existing models along these lines are based on simplified aerodynamics models (e.g., experimentally corrected aerodynamic coefficients), which limits the applicability of such low-order models in early design stages. In this work, a semi-analytical model of flexible aircraft is established through the combination of the dynamics of elastic body and the numerical linearization of high-order structure and aerodynamics models. The proposed model is derived in the body-fixed axes formulation, represents full flight dynamics (both longitudinal and lateral), and preserves the physical meanings for the states and all the derived terms. Static residualization is also adopted to enhance the model accuracy with limited number of elastic states. Using the proposed approach, low-order semi-analytical models are exemplified for different complexity aircraft representations and verified against the corresponding nonlinear high-order models.

Nomenclature

$C_{\beta T}$, $C_{\eta T}$	=	matrices linking the vector of thrust force F_{T} to $\{F_{\mathrm{thrust}}^{\top},\ M_{\mathrm{thrust}}^{\top}\}^{\top}$, and Q_{thrust}
$C_{\beta 0}$, $C_{\eta 0}$	=	aerodynamic forces on the rigid-body and flexible states at a selected trim condition, normalized by $\bar{q}$
$C_{\beta\beta}$, $C_{\beta\eta}$, $C_{\beta\dot{\eta}}$, $C_{\beta\delta}$	=	linearization coefficients of $\{F_{\mathrm{aero}}^{\top},\ M_{\mathrm{aero}}^{\top}\}^{\top}$, normalized by $\bar{q}$
$\bar{C}_{\beta\beta}$, $\bar{C}_{\beta\eta}$, $\bar{C}_{\beta\dot{\eta}}$, $\bar{C}_{\beta\delta}$	=	low-dimension modifications of $C_{\beta\beta}$, $C_{\beta\eta}$, $C_{\beta\dot{\eta}}$, $C_{\beta\delta}$ considering residualization
$C_{\eta\beta}$, $C_{\eta\eta}$, $C_{\eta\dot{\eta}}$, $C_{\eta\delta}$	=	linearization coefficients of Q_{aero}, normalized by $\bar{q}$

*Post-doctoral Fellow, Department of Aerospace Engineering. Currently: Assistant Professor, Department of Mechanical and Aerospace Engineering, The Hong Kong University of Science and Technology, Hong Kong SAR, China, AIAA Member, duan@ust.hk.
†Clarence L. (Kelly) Johnson Professor, Department of Aerospace Engineering, AIAA Fellow, cesnik@umich.edu.
‡Professor, Department of Aerospace Engineering, AIAA Associate Fellow, ilya@umich.edu.
§Loads and Aeroelastics Engineer, Flight Physics.

$\bar{C}_{\eta\beta}, \bar{C}_{\eta\eta}, \bar{C}_{\eta\dot{\eta}}, \bar{C}_{\eta\delta}$	=	low-dimension modifications of $C_{\eta\beta}, C_{\eta\eta}, C_{\eta\dot{\eta}}, C_{\eta\delta}$ considering residualization
D_k	=	matrix linking change of η to e_k
$e_k, e_{0,k}$	=	vector of kth thrust force direction with and without aircraft deformation
$E(x), f_E(x), g_E(x)$	=	complete nonlinear dynamics satisfying $E(x)\dot{x} = f_E(x) + g_E(x)u$
$\mathcal{F}_B, \mathcal{F}_I$	=	body-fixed and inertial reference frames
$F_{\mathrm{T}}, F_{\mathrm{T},k}$	=	vector of scalar thrust forces and its kth element, N
F_{Frame}	=	translational force components due to $\mathcal{F}_B$ movement (similar definitions for F_{Relative}, F_{Euler}, F_{Coriolis}, $F_{\mathrm{Centripetal}}$, F_{Ext}, F_{g}, F_{thrust}, F_{aero}), N
g, g_h	=	gravitation vector in $\mathcal{F}_B$ and gravitational constant as a function of altitude, $\mathrm{m{\cdot}s^{-2}}$
$H(\eta), H_i(\eta)$	=	matrix linking $\ddot{\eta}$ to M_{Relative} and its ith column, $\mathrm{N{\cdot}m{\cdot}s^2}$
$H_i^{(0)}, \nu_{ij}$	=	zeroth-order and first-order coefficients of $H_i(\eta)$, $\mathrm{N{\cdot}m{\cdot}s^2}$
$I_B(\eta), I_B^{(0)}$	=	inertia matrix of deformed and undeformed aircraft, $\mathrm{kg{\cdot}m^2}$
$J(\eta, \dot{\eta})$	=	matrix linking 2ω to M_{Coriolis}, $\mathrm{N \cdot m \cdot s \cdot rad^{-1}}$
M, K	=	modal mass and stiffness matrix
M_{Frame}	=	rotational moment components due to $\mathcal{F}_B$ movement (similar definitions for M_{Relative}, M_{Euler}, M_{Coriolis}, $M_{\mathrm{Centripetal}}$, M_{Ext}, M_{g}, M_{thrust}, M_{aero}), N·m
M_β, M_η	=	aerodynamics coefficient modification matrices due to residualization
m	=	mass of the aircraft, kg
n, n_{T}	=	numbers of elastic modes and the thrust forces (engines)
O_B, O_I	=	origins of $\mathcal{F}_B$ and $\mathcal{F}_I$
p, q, r	=	roll, pitch, and yaw rates in $\mathcal{F}_B$, rad/s
Q_{Frame}	=	generalized force for flexible states due to $\mathcal{F}_B$ movement (similar for Q_{Relative}, Q_{Euler}, Q_{Elastic}, Q_{Coriolis}, $Q_{\mathrm{Centripetal}}$, Q_{Ext}, Q_{g}, Q_{thrust}, Q_{aero})
$\bar{q}, \bar{q}_{\mathrm{t}}$	=	dynamic pressure and its trimmed value where aerodynamic linearization is acquired, Pa
$R(\phi, \theta)$	=	transformation matrix between the rates of Euler angles and ω
$\mathbf{r}_{B/I}, \mathbf{r}_{P/B}, \mathbf{r}_{P/I}$	=	vectors from point I to B, B to P, and I to P, m
r_C, r_{C_0}	=	positions of center of mass of the deformed and undeformed aircraft in $\mathcal{F}_B$, m
$r_{\mathrm{E},k}, r_{\mathrm{E0},k}$	=	displacement of kth engine with and without aircraft deformation, m
r_P, r_{P_0}, e_{P_0}	=	deformed, undeformed position of Point P and their difference in $\mathcal{F}_B$, m
T	=	rotation matrix between $\mathcal{F}_B$ and $\mathcal{F}_I$
u	=	vector of combined control inputs $\{{F_{\mathrm{T}}}^\top, \delta^\top\}^\top$, N and rad

$\mathbf{v}$, ${}^{I}v$, ${}^{B}v$ (v)	=	aircraft velocity vector and its projection in $\mathcal{F}_I$ and $\mathcal{F}_B$, m/s
v_x, v_y, v_z	=	forward, lateral, and vertical speed in $\mathcal{F}_B$, m/s
x, x_t	=	state vector including rigid-body and flexible states and its trimmed value
β, β_t ,$\Delta\beta$	=	combination of the translational and rotational rigid-body states, the trimmed value where aerodynamic linearization is acquired, and their difference, m/s and rad/s
Γ_i, Π_{ij}	=	first- and second-order terms of I_B (η) with respect to η, kg·m^2
δ, δ_t ,$\Delta\delta$	=	control surface deflections, its trimmed value, and the deviation from the trim condition, rad
η, η_i	=	vector of elastic states and the ith element
η_s, η_d	=	vectors of the selected and discarded elements of η
η_t, $\Delta\eta$	=	trimmed η and the deviation from the trim
Λ, Λ_i	=	matrix linking η to the change of center of mass and its ith column, m
ρ	=	altitude dependent air density, kg/m^3
ϕ, θ, ψ	=	Euler angles, rad
ψ_i	=	ith mode shape, m
Ω_0, Ω	=	sets of undeformed and deformed points
$\boldsymbol{\omega}$, ω	=	angular velocity vector and its projection in $\mathcal{F}_B$, rad/s
s (subscript)	=	selected modes in the residualization process
d (subscript)	=	discarded modes in the residualization process

I. Introduction

In the pursuit of cost and emission reduction, modern aircraft increasingly adopt high aspect-ratio wings and lightweight structures, yielding a more flexible aircraft (FA) design. The FA design enhances the structural and aerodynamics efficiency, but poses challenges for modeling and control. Conventional controller designs use a six-degree-of-freedom (6-DOF) rigid aircraft model corrected by aerodynamic flex-to-rigid ratio and with filters to suppress the elastic modes. In FA, a more direct handling of flexible modes must be taken into account; not accounting for flexible modes often leads to low-performance controllers [1] and more severe safety issues (e.g., flutter instability) [2, 3]. On the other hand, high-order models of FA [4, 5], which combine the finite element models, aerodynamic models, and rigid-body dynamics, typically have hundreds or thousands of states, and it is challenging to use them for controller design [6]. The use of high-order models in controller design may also lead to high-order control systems that require unrealistically high-performance or high-bandwidth actuators [7]. Therefore, to facilitate controller design, low-order flexible aircraft models that capture the coupling of structural dynamics, aerodynamics, and rigid-body dynamics are needed.

The low-order models are typically obtained using one of two approaches. The top-to-bottom approach involves the use of model order reduction methods (e.g., balanced truncation [6, 8], genetic algorithms [9], Krylov-based reduction [10], etc.). This numerical approach allows for a great control of the level of approximation and the size of the final model. The top-to-bottom approaches can deal with significant complex dynamic models and have been successfully implemented in industry to model aeroelastic systems [11, 12]. However, the physical meanings of the states and physics-based model structure may be lost in the model reduction process [13]. Furthermore, the available procedures are effective for developing linear parameter varying models but are less effective for the development of models which account and include nonlinearities and reflect the effects of physical parameter variations [14]. These potential issues may complicate the controller design and tuning process (e.g., matching/interpolating models across different regions, observer design, etc.) of physical parameter variations and suffer from scalability challenges [14]. On the other hand, the bottom-to-top approach adds representations for the effects of flexibility on top of the analytical 6-DOF rigid aircraft model and thus preserves the physical meaning of the states and physics-based model structure. It yields an analytic or semi-analytical model, which can be conveniently reduced to a classical rigid aircraft dynamics model. It is this latter, bottom-to-top approach, the focus of the present paper with the motivation to provide low-order models for controller and observer designs.

The existing methods to incrementally integrate the flexible aircraft dynamics into the model are categorized based on the reference frames adopted. Early investigations of Milne [15], Canavin, and Linkins [16] exploited the concept of mean axes, which defines an orthogonal axis system with the origin at the instantaneous center of mass of the deformed body. The mean axes are oriented in a way that the free vibration modes are decoupled from the rigid-body translational and rotational motion, and thus inherited the structure of rigid aircraft models in an elegant way [2, 17]. Schmidt [18] proposed methods to characterize the elastic effects on aerodynamics forces and moments using analytical potential-flow aerodynamics coefficients. As Meirovitch and Tuzcu [19] pointed out, although the use of mean axes decoupled the inertial dynamics, the coupling effect is passed to the aerodynamic loads, which may complicate the computations. Accordingly, another commonly adopted reference frame is a body-fixed frame which has its origin at a fixed point in the aircraft. In this setting, the instantaneous center of mass is not at a constant location and the inertia tensor varies. Although the equations of motion are not inertially decoupled, the use of body-fixed axes permits to include the effect of the elastic deformations on the first- and second-mass moments of inertia, thereby potentially producing more accurate results [20]. Along these lines, Meirovitch and Tuzcu [21] followed a Lagrangian formulation used a body-fixed reference frame (referred to as "pseudo-body axes" frame) and incorporated the aerodynamics from strip theory. D'Eleuterio and Barfoot [22] used a similar energy-based approach which is applicable to general elastic bodies. Gibson et al. [23] proposed a flexible aircraft model where the dihedral angles are used to represent the flexible states. Avanzini et al. proposed a mixed Newtonian-Lagrangian approach [7] to derive the equations of motion and employed the methodology to develop a simplified FA dynamics model [24]. Building on these existing work, researchers have

also identified the scenarios where the structure deformation shows significant geometrical nonlinearity [5]. Aircraft with these geometrical nonlinear deformations are referred to as very flexible aircraft (VFA). Compared to FA, VFA typically has large deformation amplitudes, and the geometrical nonlinearity hinders the linear structural analysis [25]. The VFA modeling and control are significantly different from FA; this work focuses on the control-oriented modeling of FA.

The existing methods typically rely on simplified aerodynamics models (e.g., strip theory), which may not be satisfactory for accuracy and performance [19]. This paper builds on the bottom-to-top approach in the body-fixed axis setting and establishes a semi-analytical FA model exploiting the structural and aerodynamic linearizations of high-order models, such as in NASTRAN or in the University of Michigan's Nonlinear Aeroelastic Simulation Toolbox (UM/NAST). The main contributions of the paper include deriving the full-flight semi-analytical FA model, developing an approach to extract the aerodynamics from high-order models, and processing linearization modifications to enhance accuracy and numerical stability. The proposed semi-analytical FA model is verified with a general transport aircraft (GTA) [26] and Airbus XRF1 flexible aircraft.

The paper is organized as follows: The body-fixed equations of motion of FA in the body-fixed frame are derived in Section II. The extraction of structural and aerodynamics information from high-order models, as well as the modifications to enhance accuracy and numerical stability, are discussed in Section III. The simulation case studies of flexible aircraft GTA and XRF1 models are detailed in Section IV. The conclusion and future work are discussed in Section V.

II. Semi-Analytical Low-Order Model of Flexible Aircraft

Consider an FA with mass m, an inertial frame $\mathcal{F}_I$ with origin O_I, and a body-fixed frame $\mathcal{F}_B$ with origin O_B (arbitrary point, but usually set as the aircraft undeformed center of mass), as illustrated in Figure 1. Note that the deformation of the FA is exaggerated to highlight the deformation (such large deformation are typically categorized as very flexible aircraft). The frame $\mathcal{F}_B$ is chosen in agreement with the North-East-Down (NED) flight mechanics orientation, and is related to frame $\mathcal{F}_I$ by a 3-2-1 Euler angle rotation sequence (defined by Euler angles ϕ, θ, and ψ). The rotation matrix T is defined as

$$T = \begin{bmatrix} c(\psi)c(\theta) & c(\psi)s(\phi)s(\theta) - c(\phi)s(\psi) & s(\phi)s(\psi) + c(\phi)c(\psi)s(\theta) \\ c(\theta)s(\psi) & c(\phi)c(\psi) + s(\phi)s(\psi)s(\theta) & c(\phi)s(\psi)s(\theta) - c(\psi)s(\phi) \\ -s(\theta) & c(\theta)s(\phi) & c(\phi)c(\theta) \end{bmatrix} \tag{1}$$

where $s(\cdot)$ and $c(\cdot)$ designate $\sin(\cdot)$ and $\cos(\cdot)$ functions. The rotation matrix Eq. (1) converts the coordinates in $\mathcal{F}_B$ to the ones in $\mathcal{F}_I$. For example, with the velocity of the aircraft is defined as $\mathbf{v} = \frac{^I d}{dt}\mathbf{r}_{B/I}$, its representations in $\mathcal{F}_I$ (i.e., $^I v$)

and in $\mathcal{F}_B$ (i.e., ${}^B v$) satisfy the following relationship

$$({}^I v) = T({}^B v). \tag{2}$$

In this work, a vector is projected onto $\mathcal{F}_B$ frame without extra specification, e.g., $v = {}^B v = \{v_x, v_y, v_z\}^\top$ where v_x, v_y, and v_z represent the forward, lateral, and vertical speed in $\mathcal{F}_B$ frame.

For an arbitrary point P on the aircraft, the vectors representing its position in reference frame $\mathcal{F}_I$ and $\mathcal{F}_B$ are written as $\mathbf{r}_{P/I}$ and $\mathbf{r}_{P/B}$, respectively. They satisfy the following relationship,

$$\mathbf{r}_{P/I} = \mathbf{r}_{P/B} + \mathbf{r}_{B/I}, \tag{3}$$

where $\mathbf{r}_{B/I}$ is the inertial position of the vehicle (i.e., relative to the origin O_I of $\mathcal{F}_I$). Since, the body-fixed frame is extensively used, a simplified convention is adopted for vectors are expressed in $\mathcal{F}_B$ (i.e., $\mathbf{r}_P = \mathbf{r}_{P/B}$). The time derivatives with respect to reference frames $\mathcal{F}_I$ and $\mathcal{F}_B$ are denoted as $\frac{{}^I d}{dt}$ and $\frac{{}^B d}{dt}$, and they are linked through the transport theorem as

$$\frac{{}^I d}{dt}\mathbf{v} = \frac{{}^B d}{dt}\mathbf{v} + \boldsymbol{\omega} \times \mathbf{v}, \tag{4}$$

where $\boldsymbol{\omega}$ is the angular velocity of $\mathcal{F}_B$ with respect to $\mathcal{F}_I$. We use $\dot{\mathbf{v}}$ and $\ddot{\mathbf{v}}$ as compact forms for $\frac{{}^B d}{dt}\mathbf{v}$ and $\frac{{}^B d^2}{dt^2}\mathbf{v}$. The roll, pitch, and yaw rates are defined as p, q, and r, i.e., $\omega = \{p, q, r\}^\top$. The cross product is written as a matrix multiplication by a skew-symmetric matrix (e.g., ${}^B(\boldsymbol{\omega} \times \mathbf{v}) \cong \tilde{\omega} v$). The skew-symmetric matrix $\tilde{\omega}$ is defined as

$$\tilde{\omega} = \begin{bmatrix} 0 & -r & q \\ r & 0 & -p \\ -q & p & 0 \end{bmatrix}. \tag{5}$$

This definition of a skew-symmetric matrix applies to an arbitrary vector and and skew-symmetric matrices satisfy the properties $\tilde{\omega}^\top = -\tilde{\omega}$ and $\tilde{\omega} v = -\tilde{v}\omega$. Note that the evolution of the Euler angles can be determined from

$$\frac{{}^I d}{dt}\begin{Bmatrix} \phi \\ \theta \\ \psi \end{Bmatrix} = \underbrace{\begin{bmatrix} 1 & s(\phi)t(\theta) & c(\phi)t(\theta) \\ 0 & c(\phi) & -s(\phi) \\ 0 & \frac{s(\phi)}{c(\theta)} & \frac{c(\phi)}{c(\theta)} \end{bmatrix}}_{R(\phi,\theta)} \begin{Bmatrix} p \\ q \\ r \end{Bmatrix} \tag{6}$$

where $R(\phi, \theta)$ designates the transformation matrix.

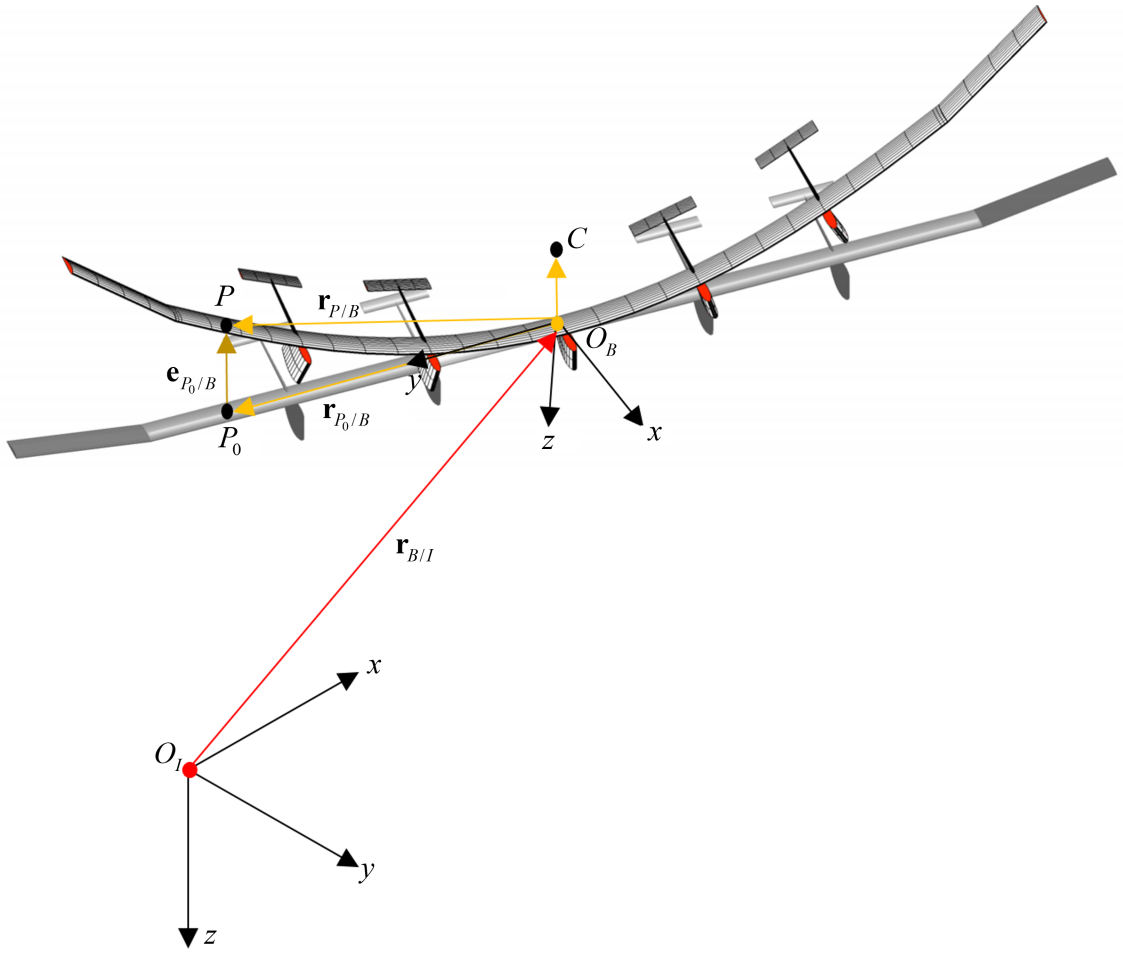

Fig. 1 Inertial and body-fixed reference frames. A typical very flexible aircraft configuration is used here just to simplify the visualization of the reference frames.

A. Equations of Motion

Flexible aircraft (FA) have moderate levels of flexibility and their structural dynamics can be characterized using linear modal analysis. Unlike VFA where the defomration displacement show significant nonlinearity, in FA formulations, the position vector of an arbitrary point r_P is decomposed into the undeformed position r_{P_0} and the elastic deformation e_{P_0} as

$$r_P = r_{P_0} + e_{P_0} = r_{P_0} + \sum_{i=1}^{n} \psi_i (P_0) \eta_i, \tag{7}$$

where $\psi_i (P_0)$ is the ith displacement mode shape at point P_0, η_i is the modal amplitude of the ith mode, and n is the number of selected modes. Define Ω_0 and Ω to be the sets of undeformed and deformed points. Then the changes in

the position of the center of mass due to deformation can be expressed as a linear function of the modal amplitudes, i.e.,

$$\begin{aligned} r_C &= r_{C_0} + \sum_{i=1}^{n} \Lambda_i \eta_i = r_{C_0} + \Lambda\eta, \\ \Lambda_i &= \frac{1}{m} \int_{P_0 \in \Omega_0} \psi_i \left(P_0\right) dm, \end{aligned} \tag{8}$$

where r_{C_0} is the position vector of the undeformed center of mass C_0, Λ_i links the ith modal amplitude to the deformation of the center of mass, $\Lambda = [\Lambda_1, \Lambda_2, ..., \Lambda_n]$ and $\eta = \{\eta_1, \eta_2, ..., \eta_n\}^\top$.

The equation of motion for a point mass m_P in reference frame $\mathcal{F}_B$ is written as

$$m_P \left(\underbrace{\frac{{}^I d^2}{dt^2} r_{B/I}}_{\text{Frame}} + \underbrace{\ddot{r}_P}_{\text{Relative}} + \underbrace{\tilde{\dot{\omega}} r_P}_{\text{Euler}} + \underbrace{2\tilde{\omega}\dot{r}_P}_{\text{Coriolis}} + \underbrace{\tilde{\omega}^2 r_P}_{\text{Centripetal}} \right) = F_P, \tag{9}$$

where F_P is the external force applied to the point mass. Note that acceleration terms are categorized into different classes: the inertial term due to the moving frame $\mathcal{F}_B$ is denoted as "Frame"; the inertial term relative to frame $\mathcal{F}_B$ is denoted as "Relative"; the other terms are Euler, Coriolis, and centripetal terms. The integration of Eq. (9) with corresponding multipliers yields the translation, rotation, and elastic equations of motion for the FA. This classification of acceleration terms is crucial as it leads all the following decomposition of translational, rotational, and flexible terms. The multipliers for translation, rotation, and elastic equations are 1, $\tilde{r}_P$, and $\psi_i^\top$, respectively.

The translation EOM is written as

$$F_{\text{Frame}} + F_{\text{Relative}} + F_{\text{Euler}} + F_{\text{Coriolis}} + F_{\text{Centripetal}} = F_{\text{Ext}}, \tag{10}$$

where F_{Ext} represents the integral of the external forces applied to the FA, while F_{Frame}, F_{Relative}, F_{Euler}, F_{Coriolis}, and $F_{\text{Centripetal}}$ represent the integrals of corresponding terms in Eq. (9). These latter terms, by exploiting Eq. (8), are derived as

$$F_{\text{Frame}} = \int_{P \in \Omega} \left(\frac{{}^I d^2}{dt^2} r_{B/I} \right) dm = m \frac{{}^I d}{dt} v = m \left(\dot{v} + \tilde{\omega} v \right), \tag{11}$$

$$F_{\text{Relative}} = \int_{P \in \Omega} \ddot{r}_P dm = m\Lambda\ddot{\eta}, \tag{12}$$

$$F_{\text{Euler}} = \int_{P \in \Omega} \tilde{\dot{\omega}} r_P dm = -m\tilde{r}_C(\eta)\dot{\omega}, \tag{13}$$

$$F_{\text{Coriolis}} = \int_{P \in \Omega} 2\tilde{\omega}\dot{r}_P dm = 2m\tilde{\omega}\Lambda\dot{\eta}, \tag{14}$$

$$F_{\text{Centripetal}} = \int_{P\in\Omega} \tilde{\omega}^2 r_P dm = m\tilde{\omega}^2 r_C(\eta). \tag{15}$$

Although the corresponding force terms in Eqs. (10) to (15) are derived for FA (assuming linear structural modal decomposition), its formulations can be used to evaluate the VFA related dynamics effects and potential error from the geometrical nonlinearity. For example, the center of mass $r_C(\eta)$ is an affine function of η for FA (assuming linear structural mode decomposition). Possible modeling errors may arise from this assumption of linear modes, particularly when FA increases flexibility towards VFA. To quantify this modeling error, an error function $e_{r_c}(\eta)$ is defined, marking the deviation of a nonlinear $r_C(\eta)$ (extracted from a high-order model) from the affine relationship defined in Eqs. (8). This deviation is typically small with small η, and gradually increases with larger η. Note from Eqs. (10) to (15) that this error function $e_{r_c}(\eta)$ directly links to the force estimation error that this model introduced due to the linear structural modes assumption. On the other hand, this error function $e_{r_c}(\eta)$ also helps establish the admissible domain of simulation (bounds on the flexible states η in simulation.

Similarly, integrating Eq. (9) with multiplier $\tilde{r}_P$, yields the rotational EOM,

$$M_{\text{Frame}} + M_{\text{Relative}} + M_{\text{Euler}} + M_{\text{Coriolis}} + M_{\text{Centripetal}} = M_{\text{Ext}} \tag{16}$$

where M_{Ext} is the external moment applied to the FA using B as the reference point. The terms M_{Frame} and M_{Relative} are given by

$$M_{\text{Frame}} = \int_{P\in\Omega} \left(\tilde{r}_P \frac{{}^I d^2}{dt^2} r_{B/I}\right) dm = m\tilde{r}_C(\eta)\left(\dot{v} + \tilde{\omega} v\right), \tag{17}$$

$$M_{\text{Relative}} = \int_{P\in\Omega} (\tilde{r}_P \ddot{r}_P) dm = H(\eta)\,\ddot{\eta}, \tag{18}$$

where $H(\eta) = [H_1(\eta), H_2(\eta), ..., H_n(\eta)]$. Each term $H_i(\eta)$ $(i = 1, 2, ..., n)$ is affine in η and cam be expressed in the form,

$$H_i(\eta) = H_i^{(0)} + \nu_{ij}\eta_j, \tag{19}$$

where

$$\begin{aligned} H_i^{(0)} &= \int_{P_0\in\Omega_0} \tilde{r}_{P_0}\psi_i(P_0)\, dm, \\ \nu_{ij} &= \int_{P_0\in\Omega_0} \left(\tilde{\psi}_j(P_0)\,\psi_i(P_0)\right) dm. \end{aligned} \tag{20}$$

From Eq. (20), it follows that $\nu_{ij} = -\nu_{ji}$. The term M_{Euler} is given by

$$M_{\text{Euler}} = \int_{P\in\Omega} \tilde{r}_P \tilde{\omega} r_P dm = I_B(\eta)\,\dot{\omega}, \tag{21}$$

where $I_B(\eta) = -\int_{P\in\Omega} \tilde{r}_P \tilde{r}_P dm$ is the inertia matrix, whose elements are second-order polynomials in η as

$$I_B(\eta) = I_B^{(0)} + \left(\Gamma_i + \Gamma_i^\top\right)\eta_i + \Pi_{ij}\eta_i\eta_j. \tag{22}$$

The term $I_B^{(0)} = -\int_{P_0\in\Omega_0} \left(\tilde{r}_{P_0}\tilde{r}_{P_0}\right) dm$ in Eq. (22) is the inertia matrix of the undeformed aircraft, and Γ_i and Π_{ij} are given by

$$\begin{aligned} \Gamma_i &= -\int_{P_0\in\Omega_0} \tilde{r}_{P_0}\tilde{\psi}_i(P_0)\,dm, \\ \Pi_{ij} &= -\int_{P_0\in\Omega_0} \tilde{\psi}_i(P_0)\,\tilde{\psi}_j(P_0)\,dm. \end{aligned} \tag{23}$$

Due to the properties of the skew-symmetric matrices, it follows that $\Pi_{ij}^\top = \Pi_{ji}$. The term M_{Coriolis} is given by

$$M_{\text{Coriolis}} = \int_{P\in\Omega} 2\tilde{r}_P\tilde{\omega}\dot{r}_P dm = 2J(\eta,\dot{\eta})\,\omega, \tag{24}$$

where

$$J(\eta,\dot{\eta}) = \left(\Gamma_i + \Pi_{ji}\eta_j\right)\dot{\eta}_i. \tag{25}$$

The term $M_{\text{Centripetal}}$ is given by

$$M_{\text{Centripetal}} = \int_{P\in\Omega} \tilde{r}_P\tilde{\omega}\tilde{\omega}r_P dm = \tilde{\omega} I_B(\eta)\,\omega, \tag{26}$$

where the right hand side is obtained from the property of the cross product ($\tilde{u}_1\tilde{u}_2\tilde{u}_2u_1 = -\tilde{u}_2\tilde{u}_1\tilde{u}_1u_2$) which holds for arbitrary vectors u_1 and u_2.

The flexible EOM is derived similarly, through the integration of Eq. (9) with multiplier $\psi_i^\top$. The dynamics of the ith mode is given by

$$Q_{\text{Frame},i} + Q_{\text{Relative},i} + Q_{\text{Elastic},i} + Q_{\text{Euler},i} + Q_{\text{Coriolis},i} + Q_{\text{Centripetal},i} = Q_{\text{Ext},i}. \tag{27}$$

The terms $Q_{\text{Frame},i}$ and $Q_{\text{Relative},i}$ are given by

$$Q_{\text{Frame},i} = \int_{P\in\Omega} \psi_i^\top \left(\frac{^I d^2}{dt^2} r_{B/I}\right) dm = m\Lambda_i^\top(\dot{v} + \tilde{\omega}v), \tag{28}$$

$$Q_{\text{Relative},i} = \int_{P\in\Omega} \psi_i^\top \ddot{r}_P dm = M_{ij}\ddot{\eta}_j, \tag{29}$$

where M_{ij} is the element of modal mass matrix M defined as

$$M_{ij} = \int_{P\in\Omega} \psi_i^\top \psi_j dm. \tag{30}$$

Similarly, define K_{ij} as the element of the modal stiffness matrix K. Then, the elastic terms are given by

$$Q_{\text{Elastic},i} = K_{ij}\eta_j. \tag{31}$$

Based on the definitions of $H_i(\eta)$, ν_{ij}, $\bar{\Gamma}_i$, and $\bar{\Pi}_{ij}$ in Eqs. (19), (20) and (23), it follows that $Q_{\text{Euler},i}$, $Q_{\text{Coriolis},i}$, and $Q_{\text{Centripetal},i}$ are given by

$$Q_{\text{Euler},i} = \int_{P\in\Omega} \psi_i^\top \tilde{\omega} r_P dm = H_i^\top(\eta)\dot{\omega}, \tag{32}$$

$$Q_{\text{Coriolis},i} = \int_{P\in\Omega} 2\psi_i^\top \tilde{\omega}\dot{r}_P dm = 2\omega^\top \nu_{ij}\dot{\eta}_j, \tag{33}$$

$$Q_{\text{Centripetal},i} = \int_{P\in\Omega} \psi_i^\top \tilde{\omega}^2 r_P dm = -\omega^\top(\Gamma_i^\top + \Pi_{ij}\eta_j)\omega. \tag{34}$$

Similar modeling error nonlinear functions due to the linear assumption are also quantifiable following the error function establishment procedure of $e_{r_c}(\eta)$ for the rotational EOM and flexible EOM. More specifically, $H(\eta)$, $I_B(\eta)$, and $J(\eta,\dot{\eta})$ are the terms that can be extracted to establish in a more general form can be extracted from high-order models. In comparison with the linear definitions, corresponding error functions $e_H(\eta)$, $e_{I_B}(\eta)$, and $e_J(\eta,\dot{\eta})$ can be established. Similar to the establishment of $e_{r_c}(\eta)$, the error due to linear assumption or the bounds of the flexible states can be established with these error functions.

B. Forces and Moments

The external forces, moments, and generalized forces are categorized into gravity, thrust, and aerodynamics components:

$$\begin{aligned} F_{\text{Ext}} &= F_{\text{g}} + F_{\text{thrust}} + F_{\text{aero}}, \\ M_{\text{Ext}} &= M_{\text{g}} + M_{\text{thrust}} + M_{\text{aero}}, \\ Q_{\text{Ext},i} &= Q_{\text{g},i} + Q_{\text{thrust},i} + Q_{\text{aero},i}. \end{aligned} \tag{35}$$

1. Gravity Forces and Moments

The gravity related terms F_{g}, M_{g}, and $Q_{\mathrm{g},i}$ are given by

$$\begin{aligned} F_{\mathrm{g}} &= mg, \\ M_{\mathrm{g}} &= \int_{P\in\Omega} (\tilde{r}_P g) dm = m\tilde{r}_C(\eta) g, \\ Q_{\mathrm{g},i} &= \int_{P\in\Omega} \left(\psi_i^\top g\right) dm = m\Lambda_i^\top g, \end{aligned} \tag{36}$$

where g is the gravity constant vector pointing to the earth. According to the transformation matrix defined in Eq. (1), g in $\mathcal{F}_B$ is given by $g = T^{-1}\{0, 0, -g_h\}^\top$, in which the gravity constant g_h is a function of the altitude.

2. Thrust Forces and Moments

Assume unit vector $e_{0,k}$ and e_k $(k = 1, 2, ..., n_{\mathrm{T}})$ represent the thrust force directions of n_{T} engines without and with deformation, respectively. Unlike in rigid aircraft where $e_{0,k} = e_k$, thrust force direction e_k in FA models is a function of η. For small deformations, the rotations due to different modes are additive so that

$$e_k = e_{0,k} + D_k \eta, \tag{37}$$

where

$$D_k = [\tilde{n}_{k,1} e_{0,k}, \tilde{n}_{k,2} e_{0,k}, ..., \tilde{n}_{k,n} e_{0,k}], \tag{38}$$

and where $n_{k,i}$ is the rotation vector at the kth engine location due to unit-amplitude ith mode. Define the thrust force of the kth engine as $F_{\mathrm{T},k}$. Then the total thrust force and moment are expressed as

$$F_{\mathrm{thrust}} = \sum_{k=1}^{n_{\mathrm{T}}} F_{\mathrm{T},k} e_k, \tag{39}$$

$$M_{\mathrm{thrust}} = \sum_{k=1}^{n_{\mathrm{T}}} F_{\mathrm{T},k} \tilde{r}_{\mathrm{E},k} e_k. \tag{40}$$

The vector $r_{\mathrm{E},k}$ represents the kth engine's displacement in the deformed configuration given by

$$r_{\mathrm{E},k} = r_{\mathrm{E}0,k} + \sum_{i=1}^{n} \psi_i \left(E_k\right) \eta_i, \tag{41}$$

where $\psi_i\left(E_k\right)$ is the ith mode shape at the kth engine location. The generalized thrust forces which appear in the dynamic equations for flexible states are calculated as

$$Q_{\text{thrust},i} = \sum_{k=1}^{n_\text{T}} F_{\text{T},k} e_k \cdot \frac{\partial r_{\text{E},k}}{\partial \eta_i} = \sum_{k=1}^{n_\text{T}} F_{\text{T},k} e_k^\top \psi_i\left(E_k\right). \tag{42}$$

In vector format, $F_\text{T} = \{F_{\text{T},1}, F_{\text{T},2}, ..., F_{\text{T},n_\text{T}}\}^\top$ and the thrust force, moment, and generalized forces are given by

$$\begin{aligned} \left\{ \begin{array}{c} F_\text{thrust} \\ M_\text{thrust} \end{array} \right\} &= C_{\beta T} F_\text{T}, \\ Q_\text{thrust} &= C_{\eta T} F_\text{T}, \end{aligned} \tag{43}$$

where

$$C_{\beta T} = \begin{bmatrix} e_1 & e_2 & ... & e_{n_\text{T}} \\ \tilde{r}_{\text{E},1} e_1 & \tilde{r}_{\text{E},2} e_2 & ... & \tilde{r}_{\text{E},n_\text{T}} e_{n_\text{T}} \end{bmatrix}, \tag{44}$$

$$C_{\eta T} = \begin{bmatrix} e_1^\top \psi_1\left(E_1\right) & e_2^\top \psi_1\left(E_2\right) & ... & e_{n_\text{T}}^\top \psi_1\left(E_{n_\text{T}}\right) \\ \vdots & \vdots & \ddots & \vdots \\ e_1^\top \psi_n\left(E_1\right) & e_2^\top \psi_n\left(E_2\right) & ... & e_{n_\text{T}}^\top \psi_n\left(E_{n_\text{T}}\right) \end{bmatrix}. \tag{45}$$

3. Aerodynamics Forces and Moments

This semi-analytical FA model exploits the linearization of high-order models to obtain characterizations of aerodynamics forces and moments. Define the vector of the rigid body states $\beta = \{v^\top, \omega^\top\}^\top$ as the combination of the translation and rotation velocity states and let δ aggregate the inputs from all control effectors.

The aerodynamics force and moment are then written as

$$\begin{aligned} \left\{ \begin{array}{c} F_\text{aero} \\ M_\text{aero} \end{array} \right\} &= \bar{q}(C_{\beta 0} + C_{\beta\beta}\Delta\beta + C_{\beta\eta}\Delta\eta + C_{\beta\dot{\eta}}\dot{\eta} + C_{\beta\delta}\Delta\delta), \\ Q_\text{aero} &= \bar{q}(C_{\eta 0} + C_{\eta\beta}\Delta\beta + C_{\eta\eta}\Delta\eta + C_{\eta\dot{\eta}}\dot{\eta} + C_{\eta\delta}\Delta\delta), \end{aligned} \tag{46}$$

where $C_{\beta 0}$ and $C_{\eta 0}$ represent the normalized aerodynamic forces affecting the rigid and flexible states at a selected trim condition, where the dynamic pressure $\bar{q} = \frac{\rho||v||^2}{2}$ (with ρ being the altitude-dependent air density) is introduced as the normalization factor. When perturbed from this selected trim condition, the aerodynamics are assumed to follow a

linear relationship around the selected trim point, where

$$\begin{aligned} \Delta\beta &= \beta - \beta_{\mathrm{t}}, \\ \Delta\eta &= \eta - \eta_{\mathrm{t}}, \\ \Delta\delta &= \delta - \delta_{\mathrm{t}} \end{aligned} \tag{47}$$

are the deviations from the corresponding trim condition values of β_{t}, η_{t}, and δ_{t}. As shown in Eq. (46), their sensitivity coefficients to the rigid states (*i.e.* $C_{\beta\beta}$, $C_{\beta\eta}$, $C_{\beta\dot{\eta}}$, and $C_{\beta\delta}$) and to the flexible states (*i.e.* $C_{\eta\beta}$, $C_{\eta\eta}$, $C_{\eta\dot{\eta}}$ and $C_{\eta\delta}$) are defined with $\bar{q}$ normalization as well. Note that more practical flexible aircraft implementation may require multiple trim points and more complex aerodynamics models. To account for these models, interpolation of the linear models or even nonlinear surrogate models can replace the simplified aerodynamics model in Eq. (46). Under those scenarios, the coefficients shown in Eq. (46) can be interpreted as the local linearizations of a more complex model to account for the aeroelastic analysis and the aerodynamic linearization matching method discussed in Section III.B.

C. Summary of the Equations of Motion

Let the state vector x aggregate the rigid body states, flexible states, Euler angles, and the position of the body-fixed frame, *i.e.*

$$x = \{\beta^\top, \eta^\top, \dot{\eta}^\top, \phi, \theta, \psi, {r_{B/I}}^\top\}^\top, \tag{48}$$

and let the n_u-dimensional control input u aggregate the thrust forces and the control surface deflections, *i.e.*

$$u = \{{F_{\mathrm{T}}}^\top, \delta^\top\}^\top. \tag{49}$$

Based on all the dynamics terms calculated in this section, the flexible aircraft dynamics are represented as

$$E(x)\dot{x} = f_E(x) + g_E(x)u \tag{50}$$

where

$$E(x) = \begin{bmatrix} mI & -m\tilde{r}_C(\eta) & 0 & m\Lambda & 0 & 0 \\ m\tilde{r}_C(\eta) & I_B(\eta) & 0 & H(\eta) & 0 & 0 \\ 0 & 0 & I & 0 & 0 & 0 \\ m\Lambda^\top & H^\top(\eta) & 0 & M & 0 & 0 \\ 0 & 0 & 0 & 0 & I & 0 \\ 0 & 0 & 0 & 0 & 0 & I \end{bmatrix}, \tag{51}$$

$$f_E(x) = \begin{Bmatrix} -m\tilde{\omega}v - 2m\tilde{\omega}\Lambda\dot{\eta} - m\tilde{\omega}^2 r_C(\eta) + mg + F_{\text{aero}}|_{\delta=0} \\ -m\widetilde{r_C}(\eta)\tilde{\omega}v - 2J(\eta,\dot{\eta})\omega - \tilde{\omega}I_B(\eta)\omega + m\tilde{r}_C(\eta)g + M_{\text{aero}}|_{\delta=0} \\ \dot{\eta} \\ -K\eta - m\Lambda^\top\tilde{\omega}v - Q_{\text{Coriolis}} - Q_{\text{Centripetal}} + m\Lambda^\top g + Q_{\text{aero}}|_{\delta=0} \\ R(\phi,\theta)\omega \\ Tv \end{Bmatrix}, \tag{52}$$

and

$$g_E(x) = \begin{bmatrix} C_{\beta T} & \bar{q}C_{\beta\delta} \\ 0_{n\times n_u} & \\ C_{\eta T} & \bar{q}C_{\eta\delta} \\ 0_{6\times n_u} & \end{bmatrix}. \tag{53}$$

III. Structural and Aerodynamics Information from High-Order Models

It is assumed that the structural modes ψ_i $(i = 1, ..., n)$ are acquired from the high-order models such as NASTRAN and UM/NAST. Note that ψ_i is the displacement-based mode shape, and other type of mode shapes (*e.g.* strain-based mode shapes in UM/NAST) should be converted to displacement mode shape with linear transformation matrices. This linear transformation is possible due to the linear deformation assumption in flexible aircraft [23]. The extraction of structural modes provides the mass matrix M, the stiffness matrix K, and mode shapes ψ_i, with which other variables Λ, $H_i^{(0)}$, Γ_i, ν_{ij}, and Π_{ij} $(i = 1, ..., n,\ j = 1, ..., n)$ are calculated accordingly. The aerodynamics coefficients are calculated based on two different scenarios. The first scenario assumes that the direct linearizations of F_{aero}, M_{aero}, and Q_{aero} with respect to the rigid states, flexible states, and control surface deflections are available, while the second scenario assumes a general state-space linear-time-invariant system realization is available. These two scenarios are detailed in

the following subsections.

A. Model-Order Reduction with Static Residualization

Assume that the high-order aerodynamic solver provides a linearization of F_{aero}, M_{aero}, and Q_{aero} at a trimmed point x_{t} with dynamic pressure $\bar{q}_{\text{t}}$. The coefficients in Eq. (46) are given by

$$\begin{aligned} C_{\beta 0} &= \frac{1}{\bar{q}_{\text{t}}} \begin{Bmatrix} F_{\text{aero,t}} \\ M_{\text{aero,t}} \end{Bmatrix}, \; C_{\beta\chi} = \frac{1}{\bar{q}_{\text{t}}} \frac{\partial}{\partial \chi} \begin{Bmatrix} F_{\text{aero}} \\ M_{\text{aero}} \end{Bmatrix}, \\ C_{\eta 0} &= \frac{Q_{\text{aero,t}}}{\bar{q}_{\text{t}}}, \; C_{\eta\chi} = \frac{1}{\bar{q}_{\text{t}}} \frac{\partial Q_{\text{aero}}}{\partial \chi}, \quad (\chi \in \{\beta, \eta, \dot{\eta}, \delta\}) \, . \end{aligned} \tag{54}$$

There are typically thousands of flexible states in the high-order models. To facilitate reduced order modeling, only a small portion of selected modes is included in our adopted aerodynamics model. Let η be decomposed according to the selected modes and the discarded modes, *i.e.*,

$$\eta = \begin{Bmatrix} \eta_{\text{s}} \\ \eta_{\text{d}} \end{Bmatrix}, \tag{55}$$

and let other matrices be also decomposed accordingly:

$$\begin{aligned} C_{\beta\eta} &= \begin{bmatrix} C_{\beta\eta,\text{s}} & C_{\beta\eta,\text{d}} \end{bmatrix}, \; C_{\beta\dot{\eta}} = \begin{bmatrix} C_{\beta\dot{\eta},\text{s}} & C_{\beta\dot{\eta},\text{d}} \end{bmatrix}, \\ C_{\eta 0} &= \begin{Bmatrix} C_{\eta 0,\text{s}} \\ C_{\eta 0,\text{d}} \end{Bmatrix}, \; C_{\eta\eta} = \begin{bmatrix} C_{\eta\eta,\text{ss}} & C_{\eta\eta,\text{sd}} \\ C_{\eta\eta,\text{ds}} & C_{\eta\eta,\text{dd}} \end{bmatrix}, \; C_{\eta\dot{\eta}} = \begin{bmatrix} C_{\eta\dot{\eta},\text{ss}} & C_{\eta\dot{\eta},\text{sd}} \\ C_{\eta\dot{\eta},\text{ds}} & C_{\eta\dot{\eta},\text{dd}} \end{bmatrix}, \; C_{\eta\delta} = \begin{bmatrix} C_{\eta\delta,\text{s}} \\ C_{\eta\delta,\text{d}} \end{bmatrix}, \\ M &= \begin{bmatrix} M_{\text{ss}} & M_{\text{sd}} \\ M_{\text{ds}} & M_{\text{dd}} \end{bmatrix}, \; K = \begin{bmatrix} K_{\text{ss}} & K_{\text{sd}} \\ K_{\text{ds}} & K_{\text{dd}} \end{bmatrix}. \end{aligned} \tag{56}$$

If the η_{d} related terms are simply discarded by setting all the matrix with subscript d to zero matrices, this could leads to significant model inaccuracy since the effects of discarded modes are not considered. As suggested in [27], steady-state responses of η_{d} can be included in the model to enhance the model accuracy, which is referred to as static residualization. To enable the residualization, the steady-state final value $\Delta\eta_{\text{d}}|_{t\to\infty}$ is calculated based on the following relationship,

$$\Delta\eta_{\text{d}}|_{t\to\infty} = \begin{bmatrix} 0 & I \end{bmatrix} \left(K - \bar{q}_{\text{t}} C_{\eta\eta}\right)^{-1} \bar{q}_{\text{t}} \left(C_{\eta\dot{\eta}} \, \Delta\dot{\eta}|_{t\to\infty} + C_{\eta\delta} \, \Delta\delta|_{t\to\infty} + C_{\eta\beta} \, \Delta\beta|_{t\to\infty}\right). \tag{57}$$

The residualization considers the effect of $\Delta\eta_{\mathrm{d}}|_{t\to\infty}$ through the modifications of the coefficients in the selected modes as

$$
\begin{aligned}
\bar{C}_{\beta\eta} &= C_{\beta\eta,\mathrm{s}},\\
\bar{C}_{\beta\dot{\eta}} &= C_{\beta\dot{\eta},\mathrm{s}} + M_\beta C_{\eta\dot{\eta}},\\
\bar{C}_{\beta\beta} &= C_{\beta\beta,\mathrm{s}} + M_\beta C_{\eta\beta},\\
\bar{C}_{\beta\delta} &= C_{\beta\delta,\mathrm{s}} + M_\beta C_{\eta\delta},\\
\bar{C}_{\eta\eta} &= C_{\eta\eta,\mathrm{ss}}\\
\bar{C}_{\eta\dot{\eta}} &= C_{\eta\dot{\eta},\mathrm{ss}} - M_\eta C_{\eta\dot{\eta}},\\
\bar{C}_{\eta\beta} &= C_{\eta\beta,\mathrm{s}} - M_\eta C_{\eta\beta},\\
\bar{C}_{\eta\delta} &= C_{\eta\delta,\mathrm{s}} - M_\eta C_{\eta\delta},
\end{aligned}
\tag{58}
$$

where the modification matrices are given by

$$
\begin{aligned}
M_\beta &= C_{\beta\eta,\mathrm{d}} \begin{bmatrix} 0 & I \end{bmatrix} \left(K - \bar{q}_{\mathrm{t}} C_{\eta\eta}\right)^{-1},\\
M_\eta &= \left(K_{\mathrm{sd}} - \bar{q}_{\mathrm{t}} C_{\eta\eta,\mathrm{sd}}\right) \begin{bmatrix} 0 & I \end{bmatrix} \left(K - \bar{q}_{\mathrm{t}} C_{\eta\eta}\right)^{-1}.
\end{aligned}
\tag{59}
$$

Low-order models of the flexible aircraft are established with these reduced-order coefficients matrices.

B. Aerodynamic Coefficients from Linearization Matching

Certain high-fidelity modeling tools (e.g., UM/NAST) provides linearized models in the state-space form. Therefore, the aerodynamics coefficients can also be acquired by matching the linearization at the trim point. This approach is similar to the modal matching concept in [28]. Define the trimmed velocity, angular rate, center of mass location, and elastic states to be v_{t}, ω_{t}, $r_{C,t}$, and η_{t},respectively. Then the linearization of the translation terms are given in Table 1. Define

$$
\Gamma_\omega = [\overline{\Gamma}_1\omega_{\mathrm{t}}, \overline{\Gamma}_2\omega_{\mathrm{t}}, ..., \overline{\Gamma}_n\omega_{\mathrm{t}}],
\tag{60}
$$

where $\overline{\Gamma}_i = \Gamma_i + \Gamma_i^\top$, $(i = 1, 2, ..., n)$ and

$$
J_\omega = [(\Gamma_1 + \Pi_{j1}\eta_{j,\mathrm{t}})\omega_{\mathrm{t}}, (\Gamma_2 + \Pi_{j2}\eta_{j,\mathrm{t}})\omega_{\mathrm{t}}, ...(\Gamma_n + \Pi_{jn}\eta_{j,\mathrm{t}})\omega_{\mathrm{t}}].
\tag{61}
$$

The rotational terms and their linearization are given in Table 2. Similarly, define matrices ν_ω and Π_ω with their individual terms given by

$$
\nu_{\omega,ij} = \omega_{\mathrm{t}}^\top \nu_{ij},
\tag{62}
$$

$$\Pi_{\omega,ij} = \omega_{\mathrm{t}}^{\top} \bar{\Pi}_{ij} \omega_{\mathrm{t}}. \tag{63}$$

The flexible terms and their linearization are given in Table 3.

Table 1 Translation terms and linearization

Terms	Expression	Linearization terms	Expression
F_{Frame}	$m\left(\dot{v} + \tilde{\omega} v\right)$	ΔF_{Frame}	$m\Delta\dot{v} + m\tilde{\omega}_{\mathrm{t}}\Delta v - m\tilde{v}_{\mathrm{t}}\Delta\omega$
F_{Inertial}	$m\Lambda\ddot{\eta}$	$\Delta F_{\text{Inertial}}$	$m\Lambda\Delta\ddot{\eta}$
F_{Euler}	$-m\tilde{r}_C(\eta)\dot{\omega}$	ΔF_{Euler}	$-m\tilde{r}_{C,\mathrm{t}}\Delta\dot{\omega}$
F_{Coriolis}	$2m\tilde{\omega}\Lambda\dot{\eta}$	$\Delta F_{\text{Coriolis}}$	$2m\tilde{\omega}_{\mathrm{t}}\Lambda\Delta\dot{\eta}$
$F_{\text{Centrifugal}}$	$m\tilde{\omega}^2 r_C\left(\eta\right)$	$\Delta F_{\text{Centrifugal}}$	$m(2\tilde{\omega}_{\mathrm{t}}\tilde{r}_{C,\mathrm{t}} + \tilde{r}_{C,\mathrm{t}}\tilde{\omega}_{\mathrm{t}})\Delta\omega + m\tilde{\omega}_{\mathrm{t}}^2\Lambda\Delta\eta$

Table 2 Rotational terms and linearization

Terms	Expression	Linearization terms	Expression
M_{Frame}	$m\tilde{r}_C(\eta)\left(\dot{v} + \tilde{\omega} v\right)$	ΔM_{Frame}	$m\tilde{r}_{C,\mathrm{t}}\Delta\dot{v} + m\tilde{r}_{C,\mathrm{t}}\tilde{\omega}_{\mathrm{t}}\Delta v - m(\tilde{\omega}_{\mathrm{t}}\tilde{v}_{\mathrm{t}} - \tilde{v}_{\mathrm{t}}\tilde{\omega}_{\mathrm{t}})\Lambda\Delta\eta - m\tilde{r}_{C,\mathrm{t}}\tilde{v}_{\mathrm{t}}\Delta\omega$
M_{Inertial}	$H\left(\eta\right)\ddot{\eta}$	$\Delta M_{\text{Inertial}}$	$H\left(\eta_{\mathrm{t}}\right)\Delta\ddot{\eta}$
M_{Euler}	$I_B\left(\eta\right)\dot{\omega}$	ΔM_{Euler}	$I_{B,\mathrm{t}}\Delta\dot{\omega} + \Gamma_{\omega}\Delta\eta$
M_{Coriolis}	$2J\left(\eta,\dot{\eta}\right)\omega$	$\Delta M_{\text{Coriolis}}$	$2J_{\omega}\Delta\dot{\eta}$
$M_{\text{Centrifugal}}$	$\tilde{\omega} I_B\left(\eta\right)\omega$	$\Delta M_{\text{Centrifugal}}$	$(\tilde{\omega}_{\mathrm{t}} I_{B,\mathrm{t}} - \widetilde{I_{B,\mathrm{t}}\omega_{\mathrm{t}}})\Delta\omega + \tilde{\omega}_{\mathrm{t}}\Gamma_{\omega}\Delta\eta$

Table 3 Flexible terms and linearization

Terms	Expression	Linearization terms	Expression
$Q_{\text{Frame},i}$	$m\Lambda_i^{\top}(\dot{v} + \tilde{\omega} v)$	ΔQ_{Frame}	$m\Lambda^{\top}(\Delta\dot{v} + \tilde{\omega}_{\mathrm{t}}\Delta v - \tilde{v}_{\mathrm{t}}\Delta\omega)$
$Q_{\text{Inertial},i} + Q_{\text{Elastic},i}$	$M_{ij}\ddot{\eta}_j + K_{ij}\eta_j$	$\Delta Q_{\text{Inertial}}$	$M\Delta\ddot{\eta} + K\Delta\eta$
$Q_{\text{Euler},i}$	$H_i^{\top}(\eta)\dot{\omega}$	ΔQ_{Euler}	$H^{\top}(\eta_{\mathrm{t}})\Delta\dot{\omega}$
$Q_{\text{Coriolis},i}$	$2\omega^{\top}\nu_{ij}\dot{\eta}_j$	$\Delta Q_{\text{Coriolis}}$	$2\nu_{\omega}\Delta\dot{\eta}$
$Q_{\text{Centrifugal},i}$	$-\omega^{\top}(\Gamma_i^{\top} + \Pi_{ij}\eta_j)\omega$	$\Delta Q_{\text{Centrifugal}}$	$-\Pi_{\omega}\Delta\eta$

Assuming small changes in Euler angles and altitudes, the state-space linearization of the system at the trim condition is given by

$$E_{\mathrm{r}}\Delta\dot{x}_{\mathrm{r}} = A_{\mathrm{r}}\Delta x_{\mathrm{r}} + B_{\mathrm{r}}\Delta u \tag{64}$$

where $\Delta x_{\mathrm{r}} = \{\Delta v^{\top}, \Delta\omega^{\top}, \Delta\eta_{\mathrm{s}}{}^{\top}, \Delta\dot{\eta}_{\mathrm{s}}{}^{\top}\}^{\top}$. The matrices E_{r} and A_{r} are given by

$$E_{\mathrm{r}} = \begin{bmatrix} mI & -m\tilde{r}_{C,\mathrm{t}} & 0 & m\Lambda \\ m\tilde{r}_{C,\mathrm{t}} & I_B\left(\eta_{\mathrm{t}}\right) & 0 & H\left(\eta_{\mathrm{t}}\right) \\ 0 & 0 & I & 0 \\ m\Lambda^{\top} & H^{\top}\left(\eta_{\mathrm{t}}\right) & 0 & M \end{bmatrix} \tag{65}$$

$$A_{\mathrm{r}} = A_{\mathrm{r0}} + \bar{q}\begin{bmatrix} \bar{C}_{\beta\beta} & \bar{C}_{\beta\eta} & \bar{C}_{\beta\dot{\eta}} \\ & 0_{n\times(2n+6)} & \\ \bar{C}_{\eta\beta} & \bar{C}_{\eta\eta} & \bar{C}_{\eta\dot{\eta}} \end{bmatrix} \tag{66}$$

where

$$A_{\mathrm{r0}} = \begin{bmatrix} -m\tilde{\omega}_{\mathrm{t}} & m(\tilde{v}_{\mathrm{t}} - 2\tilde{\omega}_{\mathrm{t}}\tilde{r}_{C,\mathrm{t}} - \tilde{r}_{C,\mathrm{t}}\tilde{\omega}_{\mathrm{t}}) & -m\tilde{\omega}_{\mathrm{t}}^2\Lambda & -2m\tilde{\omega}_{\mathrm{t}}\Lambda \\ -m\tilde{r}_{C,\mathrm{t}}\tilde{\omega}_{\mathrm{t}} & m\tilde{r}_{C,\mathrm{t}}\tilde{v}_{\mathrm{t}} - (\tilde{\omega}_{\mathrm{t}}I_{B,\mathrm{t}} - \widetilde{I_{B,\mathrm{t}}\omega_{\mathrm{t}}}) & m(\tilde{\omega}_{\mathrm{t}}\tilde{v}_{\mathrm{t}} - \tilde{v}_{\mathrm{t}}\tilde{\omega}_{\mathrm{t}})\Lambda - \Gamma_{\omega} + \tilde{\omega}_{\mathrm{t}}\Gamma_{\omega} & -2J_{\omega} \\ 0 & 0 & 0 & I \\ -m\Lambda^{\top}\tilde{\omega}_{\mathrm{t}} & m\Lambda^{\top}\tilde{v}_{\mathrm{t}} & \Pi_{\omega} - K & -2\nu_{\omega} \end{bmatrix} \tag{67}$$

The matrix B_{r} is given by

$$B_{\mathrm{r}} = \begin{bmatrix} C_{\beta T} & \bar{q}\bar{C}_{\beta\delta} \\ 0_{n\times n_u} & \\ C_{\eta T} & \bar{q}\bar{C}_{\eta\delta} \end{bmatrix}. \tag{68}$$

Assuming a reduced order linear state space model is available from higher order modeling model order reduction with A_{ref}, B_{ref} matrices, the aerodynamic coefficients are acquired through matching ${E_{\mathrm{r}}}^{-1}A_{\mathrm{r}}$ to A_{ref}, and matching ${E_{\mathrm{r}}}^{-1}B_{\mathrm{r}}$ to B_{ref}. Additional terms $C_{\beta 0}$ and $C_{\eta 0}$ are defined by the zero state time rate of change condition at the trim condition. This linearization formula from Eq. (64) to (68) also helps in evaluating the modeling error in the residualization procedure due to discarding modes. All the residualization related terms $\bar{C}_{\beta\eta}$, $\bar{C}_{\beta\eta}$, $\bar{C}_{\beta\dot{\eta}}$, $\bar{C}_{\beta\beta}$, $\bar{C}_{\beta\delta}$, $\bar{C}_{\eta\eta}$, $\bar{C}_{\eta\dot{\eta}}$, $\bar{C}_{\eta\dot{\eta}}$, $\bar{C}_{\eta\dot{\eta}}$, $\bar{C}_{\eta\dot{\eta}}$, $\bar{C}_{\eta\beta}$, $\bar{C}_{\eta\delta}$ can be generated with different numbers of discarded modes, and the corresponding frequency-domain modeling error due to residualization can be generated by generating the frequency response function of Eq. (64).

IV. Simulation Case Studies

A. Case Studies with a General Transport Aircraft

The proposed semi-analytical FA model is numerically verified in this section for a general transport aircraft, which weights 7139.74 kg and has a 19-m wingspan. The UM/NAST beam-based model is selected to be the high-order benchmark model, which is shown in Figure 2. The detailed process of creating this model is described in [29]. The nonlinear UM/NAST model has 333 states, including 13 rigid states and 320 elastic states, considering the flexibility of the wings and the fuselage. The GTA weighs 7139.74 kg, and the aerodynamics linearization is acquired at a trimmed cruise flight at the altitude of 6096 m and speed of 160 m/s. At this flight condition, the trimmed angle of attack is 1.345°.

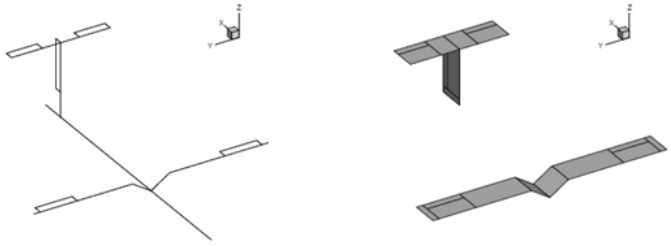

Fig. 2 General transport aircraft UM/NAST modeling [29].

Three representative test cases are designed to show the longitudinal, lateral, and coupled responses of the semi-analytical modeling of GTA. The excitations are defined as follows:

- a longitudinal excitation from elevator doublet with 1-degree amplitude,
- a lateral excitation from aileron doublet with 1-degree amplitude, and
- a coupled excitation of elevator and aileron with 1-degree amplitude.

The doublets inputs are illustrated in Figure 3. In the first two excitations, the doublets are introduced with $t_{\text{start}} = 1$ second, $t_{\text{half}} = 4$ seconds and $t_{\text{end}} = 7$ seconds. In the coupled excitation, an identical elevator doublet profile is introduced while the aileron doublet is introduced 1 second later such that the contributions to the aircraft responses are more distinguishable. The translation velocities (v_x, v_y, and v_z), rotation velocities (p, q, and r), Euler angles (ϕ, θ, and ψ), and representative elastic states are shown in Figures 4-6. To evaluate the aeroelastic behavior, 4 elastic modes ($n = 4$) are preserved in the proposed low-order semi-analytical model. The first out-of-plane bending modes at 1.48 Hz are most dominant in this configuration, thus, the amplitudes of these modes on the left and right wings (η_L and η_R) are selected to represent the responses of the flexible states. Under linearity assumption, unity values of η_L and η_R correspond to the wing tip upward deflection of 0.11 m.

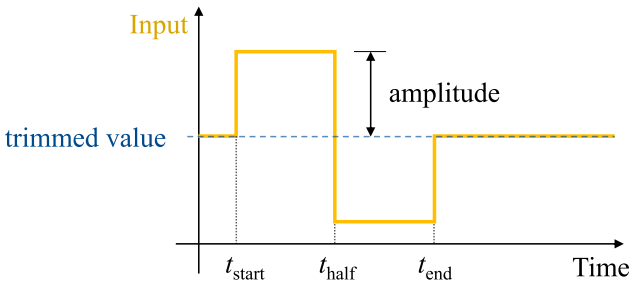

Fig. 3 Input doublet profile.

The rigid body and incremental out-of-plane bending modal responses under 1-degree elevator doublet input, using high-order UM/NAST and proposed semi-analytical modeling with/without residualization (in Section III.A), are shown in Figure 4. The primary responses to this longitudinal excitation are the forward velocity v_x, vertical velocity v_z, pitch

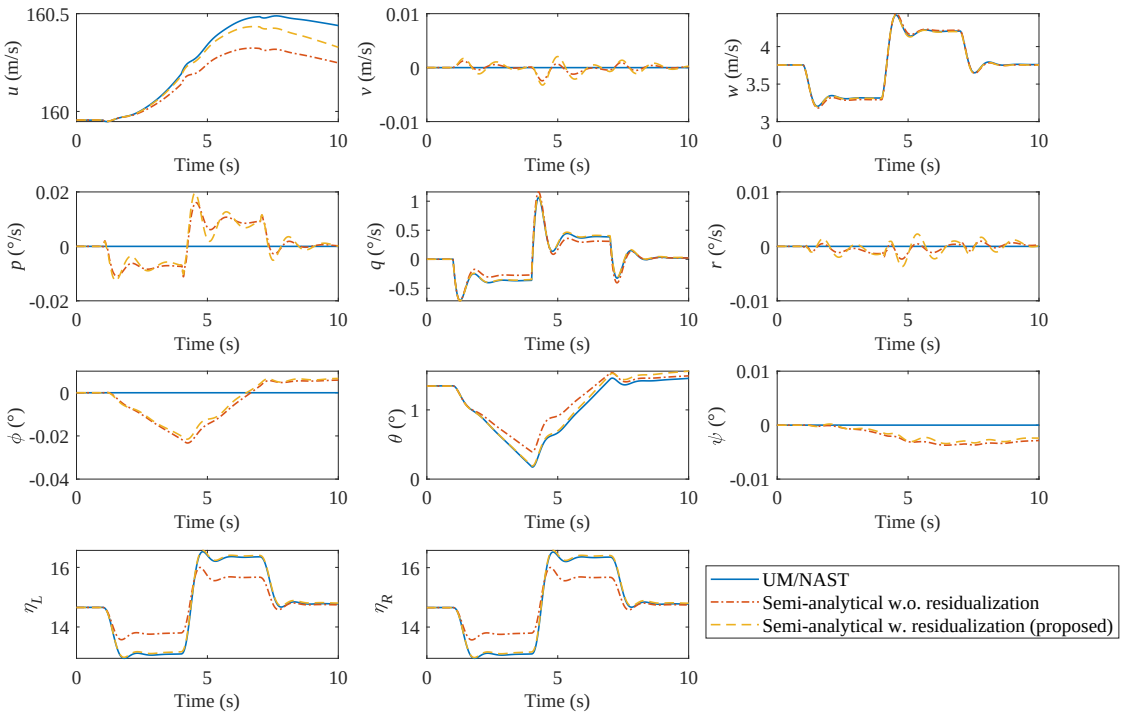

Fig. 4 Rigid body and out-of-plane bending modal responses of GTA under 1-degree elevator doublet input.

rate q, and pitch angle θ. The proposed semi-analytical model responses match the UM/NAST responses, especially with the proposed residualization. For the rest of the lateral responses, small deviations are observed for the proposed semi-analytical models. This is attributed to the significantly fewer numbers of modes (less than 10%) being used as compared to the high-order models and small spill-over effects unavoidable with any model order reduction. Despite these small deviations, the out-of-plane bending modes $\Delta\eta_L$ and $\Delta\eta_R$ are very accurately captured. In the simulated descending maneuver, the bending modal amplitudes follow the doublet sequence, and the responses on the left and right wings are symmetrical.

The rigid body and incremental out-of-plane bending modal responses under 1-degree aileron doublet input are shown in Figure 5. The primary responses to this input are the lateral velocity v_y, the roll rate p, the yaw rate r, the roll angle ϕ, and the yaw angle ψ. These lateral terms are quite off for the semi-analytical model without residualization, however, they are more accurately captured with residualization. Unlike the longitudinal responses in Figure 4, the response for this lateral excitation introduces anti-symmetrical modal responses on the left and right wings. Note that slight constant deviation arises from the small trim difference between the proposed semi-analytical model and the high-order UM/NAST model, but the trend due to dynamics are captured. The residualization is observed to not only affects the elastic responses but also has a significant impact on the rigid body responses. The out-of-plane bending

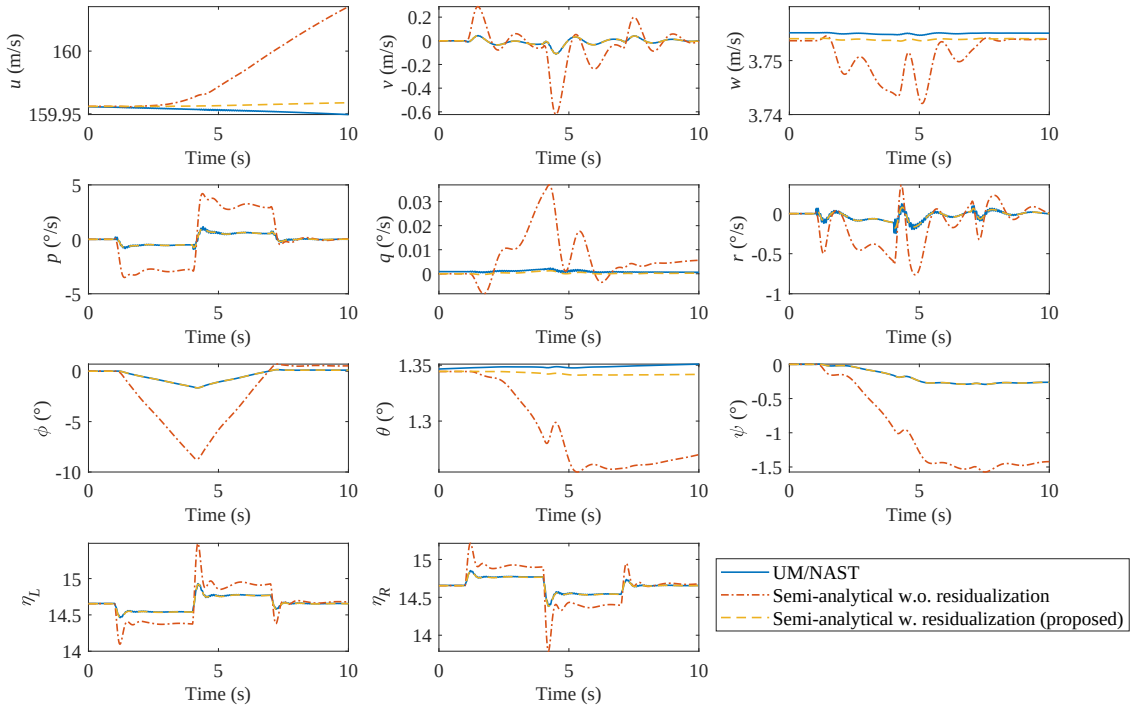

Fig. 5 Rigid body and out-of-plane bending modal responses of GTA under 1-degree aileron doublet input.

terms $\Delta\eta_L$ and $\Delta\eta_R$ are very accurately captured. Unlike the longitudinal responses in Figure 4, the response for this lateral excitation introduces anti-symmetrical modal responses on the left and right wings.

The responses to 1-degree coupled doublet input are shown in Figure 6, which further confirm that the semi-analytical model with residualization captures the dynamics of the high-order UM/NAST mode with significantly fewer states. This coupled excitation response has both the longitudinal and lateral excitations to the FA. The longitudinal excitation mainly introduces lift and pitch moment to the aircraft, while the lateral excitation introduces mainly roll moment to the aircraft. This effect of coupled excitations is well observed in the simulated responses in Figure 6. Also, the out-of-plane bending terms $\Delta\eta_L$ and $\Delta\eta_R$ are very accurately captured. The responses' major contribution arises from the longitudinal excitation as it introduces lift, but the characteristic drop of $\Delta\eta_R$ at around 5 second is also accurately captured, indicating the effectiveness of the semi-analytical model.

To further analyze the modeling error of the proposed semi-analytical method, the integrated square of the response error normalized by the total responses (away from the trim) is selected as a model accuracy metric. These normalized

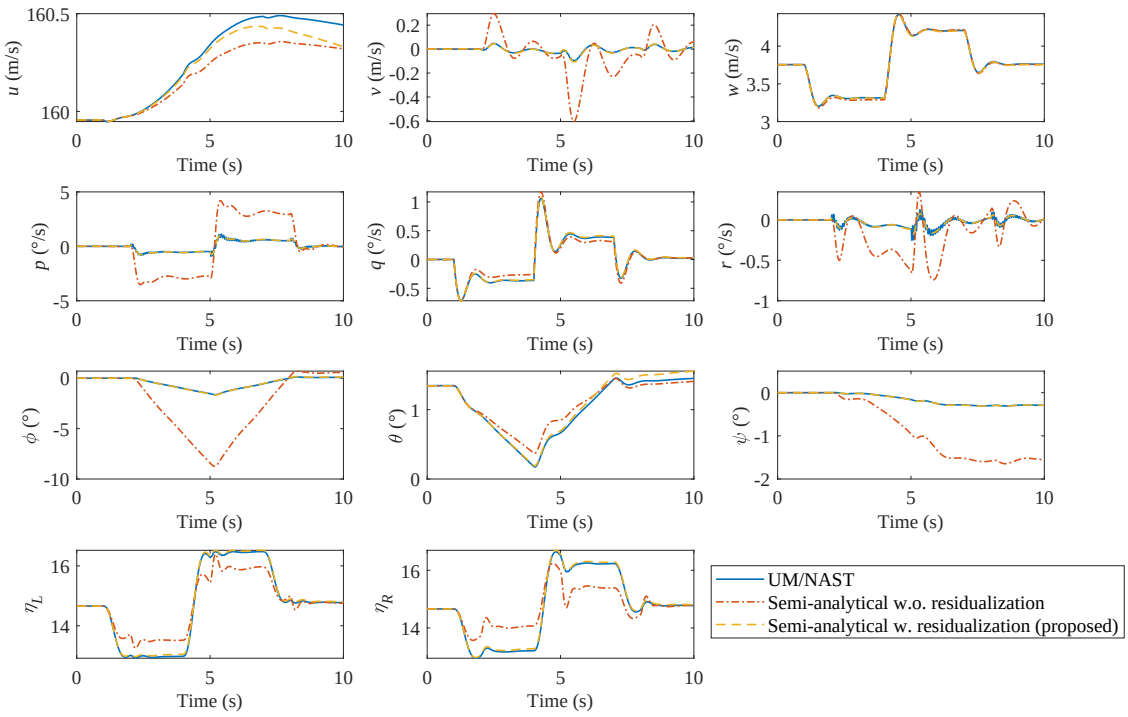

Fig. 6 Rigid body and out-of-plane bending modal responses of GTA under 1-degree coupled doublet input.

errors for the rigid-body states, flexible states, and all states of interests are defined as e_{r}, e_{f}, and e_{all}; they are given by

$$
\begin{aligned}
e_{\mathrm{r}} &= \frac{\int_0^{T_{\mathrm{sim}}} \left| y_{\mathrm{r,NAST}}(t) - y_{\mathrm{r,ROM}}(t) \right|^2 dt}{\int_0^{T_{\mathrm{sim}}} \left| y_{\mathrm{r,NAST}}(t) \right|^2 dt}, \\
e_{\mathrm{f}} &= \frac{\int_0^{T_{\mathrm{sim}}} \left| y_{\mathrm{f,NAST}}(t) - y_{\mathrm{f,ROM}}(t) \right|^2 dt}{\int_0^{T_{\mathrm{sim}}} \left| y_{\mathrm{f,NAST}}(t) \right|^2 dt}, \\
e_{\mathrm{all}} &= \frac{\int_0^{T_{\mathrm{sim}}} \left| y_{\mathrm{NAST}}(t) - y_{\mathrm{ROM}}(t) \right|^2 dt}{\int_0^{T_{\mathrm{sim}}} \left| y_{\mathrm{NAST}}(t) \right|^2 dt},
\end{aligned}
\tag{69}
$$

where $T_{\mathrm{sim}} = 10$ is the simulation time, while $y_{\mathrm{r,NAST}}$ and $y_{\mathrm{r,ROM}}$ are the rigid body states of interest (*i.e.* $\Delta\boldsymbol{\beta}$, $\Delta\phi$, $\Delta\theta$, and $\Delta\psi$) for UM/NAST and the proposed semi-analytical reduced order model, respectively. Same notion applies to the flexible states ($y_{\mathrm{f,NAST}}$ and $y_{\mathrm{f,ROM}}$) and total states (y_{NAST} and y_{ROM}). The errors are evaluated based on the deviation of the responses from the the trim condition such that only the dynamic response differences are compared. Figure 7 illustrates the modeling error for the three different test cases with increasing excitation amplitudes. The presented percentage exaggerate the model inaccuracy in a way that the high-frequency oscillations in the UM/NAST model are intentionally discarded in the semi-analytical model, while these high-frequency error contributes to the total

error integration in Eq. (69). The lateral excitation results in a relatively low modeling error (below 6%) while the longitudinal and coupled excitation exhibit an increasing modeling error with increasing amplitudes. This attributes to the fact the increased geometrical nonlinearity, which is not captured in our the flexible aircraft modeling framework. In the maximum amplitudes shown in Figure 7, the tip deflection reaches about 3.7 m, which is more than one-third of the total wingspan. Even with this large deformation violating the linear assumption, the proposed semi-analytical model still captures more than 80% of the dynamic response.

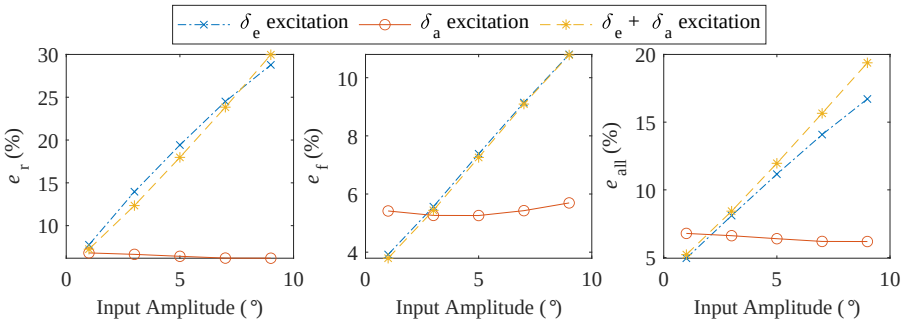

Fig. 7 Normalized error of the rigid-body states, flexible states, and all states for the longitudinal excitation, lateral excitation, and the coupled excitation for different amplitudes.

To understand the effect of the number of the elastic states, random coupled doublet excitations from the elevators, ailerons, rudder, and thrust input are generated and the model accuracy is assessed. The thrust forces are kept to have maximum amplitudes of 1000 N, and the control surface deflections have maximum of 1 degree. The statistics of the modeling error of the rigid-body states, the flexible states, and all the states are shown in Figure 8. Note that only the statistics for $n = 2, 4, 6, 7, 9, 11, 12, 14, 16, 18, 20$ are presented. This selection is rationalized by the fact that the 7th and the 11th modes are elastic modes of the fuselage, and that the symmetric modes of the left and right wings are always preserved in the proposed semi-analytical approach. In this GTA setup, the first two bending modes are dominant such that considering only two elastic states yields relatively accurate results with residualization. However, same level of modeling accuracy requires almost 18 elastic states without residualization. Also, the modeling error uncertainty is reduced with the proposed residualization.

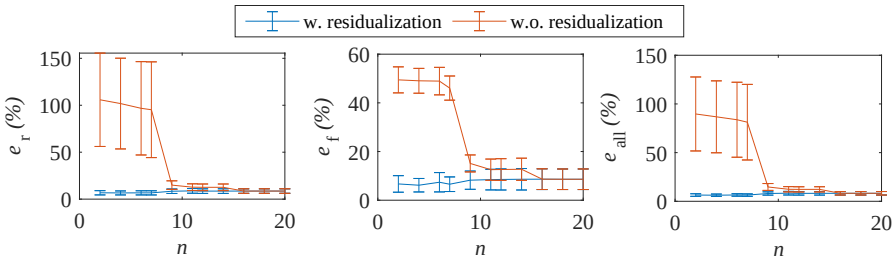

Fig. 8 Normalized error of the rigid-body states, flexible states, and all states for different number of preserved elastic modes of GTA, with and without residualization.

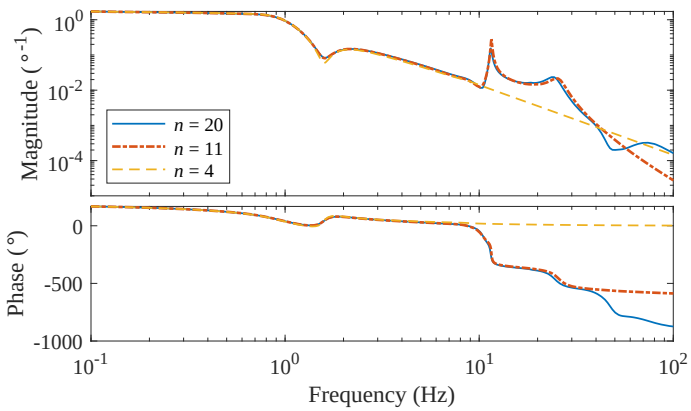

Fig. 9 Frequency-domain responses of GTA's elevator input to the first bending mode amplitudes, with residualization keeping different numbers of flexible modes.

As discussed in Section III.B, the frequency-domain system representations can be used to analyze the modeling error due to the residualization procedure. This has been verified by comparing the frequency response function (FRF) of FA from the joint elevator incremental input in degrees to the flexible responses. The FRF with 20, 11, and 4 kept modes with corresponding cutoff frequencies at 63.19 Hz, 20.85 Hz, and 8.13 Hz, respectively, are shown in Figure 9. The effect of the residualization is clearly shown as the low-frequency portions of the responses are kept the same due to the consideration of DC component preservation in the residualization procedure. The frequency ranges that the proposed FA model has relatively high accuracy can be well estimated from the modal decomposition information. It is also shown that the cutoff frequency is a desirable indicator of the frequencies, beyond which significant deviations exists.

B. Case Studies with XRF1 Flexible Aircraft

In this section, the proposed semi-analytical approach is applied to a representative commercial transport aircraft. The XRF1 is an Airbus provided industrial standard multi-disciplinary research test case representing a typical configuration for a long range wide body aircraft. The UM/NAST model of the XRF1 [30] shown in Figure 10 is used as a reference full-order solution. The nonlinear UM/NAST model of the XRF1 has 1021 states, including 13 rigid states and 1008 elastic states. The XRF1 weighs 7139.74 kg, and it is trimmed at an altitude of 8484.108 m and speed of 253.9825 m/s (*i.e.*, Mach 0.83). The trimmed angle of attack is 1.315°.

The responses to the coupled excitation (third test case as in Section IV.A) of 1-degree amplitude using 10 elastic states are shown in Figure 11. Clearly, the proposed semi-analytical model captures the dynamics with residualization. In this descending turn maneuver, the roll rate and angle are very accurately captured. The pitch and yaw responses have slight error but the trend is mostly captured. The modeling errors for different numbers of elastic modes are shown

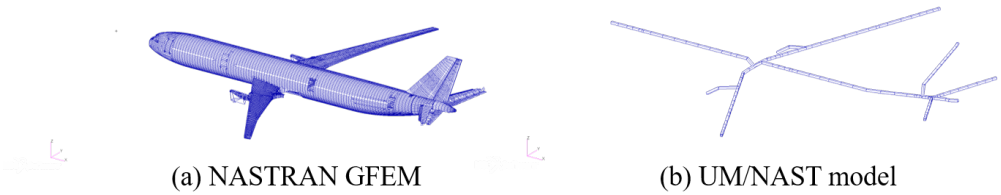

(a) NASTRAN GFEM (b) UM/NAST model

Fig. 10 XRF1 NASTRAN GFEM model and UM/NAST model [30]

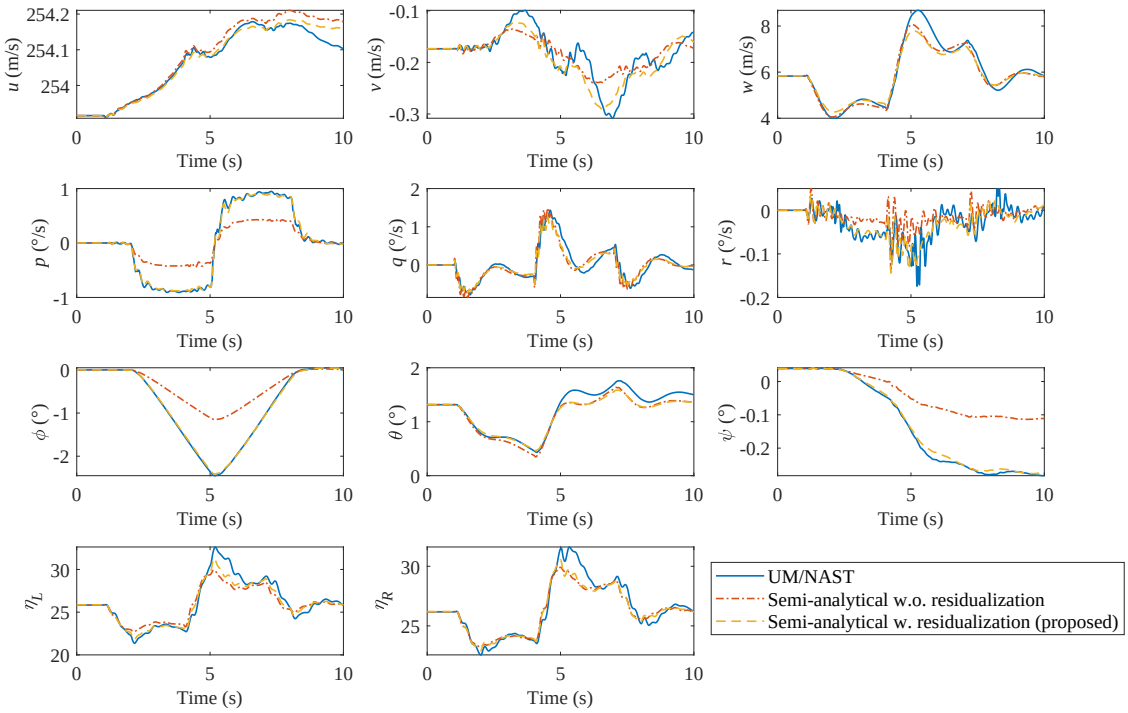

Fig. 11 Rigid body and out-of-plane bending modal responses of XRF1 under 1-degree coupled doublet input.

in Figure 12. The modeling error is higher in the case of XRF1 than GTA since the XRF1 responses contains more high-frequency components, which exaggerate the error metrics. Also, more states are discarded in the XRF1 model such that the modeling error is higher than in the case of the GTA model. In particular, having more than 14 states can further enhance the model accuracy both with and without residualization. Also, the residualization reduces the total modeling error by about 30%.

V. Conclusion

This paper introduced a semi-analytical low-order model of the flight dynamics of flexible aircraft, where the geometric displacements, although in the linear range, cannot be accurately captured only by flex-to-rigid ratio correction

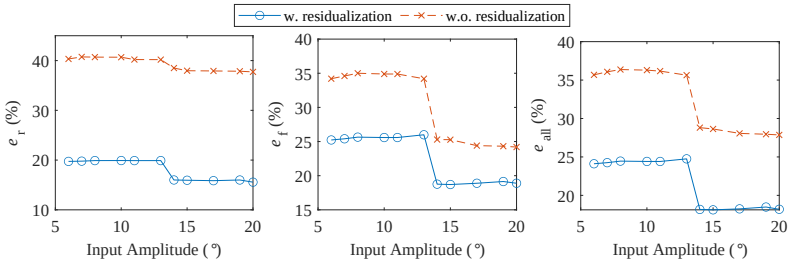

Fig. 12 Normalized error of the rigid-body states, flexible states, and all states for different number of preserved elastic modes of XRF1, with and without residualization.

of aerodynamic effects in the 6-rigid-DOF equations of motion. It adopted the body-fixed axes formulation and the flexible aircraft dynamics were derived including rigid and flexible degrees of freedom and preserving the physical interpretation of the various parameters in the problem. The aerodynamic linearization from high-order models was employed to enhance the modeling accuracy. To enhance the model accuracy with fewer states, static residualization was also derived and adopted. In addition, the analytical linearization of the model was derived, as well as methods to extract the aerodynamic linearization from the state-space linear-time-invariant system realization. The new approach was verified for modeling a general transport aircraft and an Airbus XRF1 aircraft. Both longitudinal, lateral, and coupled dynamics were well captured with significantly less number of states in comparison to reference high-order nonlinear UM/NAST models.

Acknowledgements

The authors would like to thank Airbus for providing the XRF1 test case as a mechanism for demonstration of the approaches presented in this paper. The authors would also like to thank Guillaume Dematt'e (University of Michigan, currently at Safran) for his initial insights in support to this study. The material of this paper is based upon work supported by Airbus in the frame of the Airbus-Michigan Center for Aero-Servo-Elasticity of Very Flexible Aircraft (CASE-VFA).

References

[1] Silvestre, F. J., Guimarães Neto, A. B., Bertolin, R. M., da Silva, R. G. A., and Paglione, P., "Aircraft control based on flexible aircraft dynamics," *Journal of Aircraft*, 2017, pp. 262–271.

[2] Schmidt, D. K., and Raney, D. L., "Modeling and simulation of flexible flight vehicles," *Journal of Guidance, Control, and Dynamics*, Vol. 24, No. 3, 2001, pp. 539–546. doi:10.2514/2.4744.

[3] Tuzcu, I., and Meirovitch, L., "Effects of flexibility on the stability of flying aircraft," *Journal of Dynamic Systems, Measurement, and Control*, Vol. 127, No. 1, 2005, pp. 41–49. doi:10.1115/1.1870040.

[4] Shearer, C. M., and Cesnik, C. E. S., "Nonlinear flight dynamics of very flexible aircraft," *Journal of Aircraft*, Vol. 44, No. 5, 2007, pp. 1528–1545. doi:10.2514/1.27606.

[5] Su, W., and Cesnik, C. E. S., "Nonlinear aeroelasticity of a very flexible blended-wing-body aircraft," *Journal of Aircraft*, Vol. 47, No. 5, 2010, pp. 1539–1553. doi:10.2514/1.47317.

[6] Pereira, M. F., Duan, M., Cesnik, C. E. S., Kolmanovsky, I., and Vetrano, F., "Model Predictive Control for Very Flexible Reduced-Order Models," *International Forum on Aeroelasticity and Structural Dynamics*, 2022.

[7] Avanzini, G., Capello, E., and Piacenza, I. A., "Mixed Newtonian–Lagrangian approach for the analysis of flexible aircraft dynamics," *Journal of Aircraft*, Vol. 51, No. 5, 2014, pp. 1410–1421. doi:10.2514/1.C032235.

[8] Wang, Y., Song, H., Pant, K., Brenner, M. J., and Suh, P. M., "Model order reduction of aeroservoelastic model of flexible aircraft," *57th AIAA/ASCE/AHS/ASC Structures, Structural Dynamics, and Materials Conference*, 2016, p. 1222.

[9] Zhu, J., Wang, Y., Pant, K., Suh, P. M., and Brenner, M. J., "Genetic algorithm-based model order reduction of aeroservoelastic systems with consistent states," *Journal of aircraft*, Vol. 54, No. 4, 2017, pp. 1443–1453.

[10] Goizueta, N., Wynn, A., and Palacios, R., "Parametric Krylov-based order reduction of aircraft aeroelastic models," *AIAA Scitech 2021 Forum*, 2021, p. 1798.

[11] Gadient, R., Lavretsky, E., and Wise, K., "Very Flexible Aircraft Control Challenge Problem," *AIAA Guidance, Navigation, and Control Conference*, Minneapolis, Minnesota, 2012.

[12] Zimmer, M., Feldwisch, J. M., and Ritter, M. R., "Coupled CFD-CSM Analyses of a Highly Flexible Transport Aircraft by Means of Geometrically Nonlinear Methods," *International Forum on Aeroelasticity and Structural Dynamics*, 2022.

[13] Lanchares, M., Kolmanovsky, I., Cesnik, C. E. S., and Vetrano, F., "Model order reduction for coupled nonlinear aeroelastic-flight mechanics of very flexible aircraft," *International Forum on Aeroelasticity and Structural Dynamics*, Savannah, Georgia, 2019.

[14] Lu, K., Zhang, K., Zhang, H., Gu, X., Jin, Y., Zhao, S., Fu, C., and Yang, Y., "A review of model order reduction methods for large-scale structure systems," *Shock and Vibration*, Vol. 2021, 2021, pp. 1–19.

[15] Milne, R. D., *Dynamics of the deformable aeroplane*, HM Stationery Office, 1964.

[16] Canavin, J. R., and Likins, P. W., "Floating reference frames for flexible spacecraft," *Journal of Spacecraft and Rockets*, Vol. 14, No. 12, 1977, pp. 724–732. doi:10.2514/3.57256.

[17] Keyes, S. A., Seiler, P., and Schmidt, D. K., "Newtonian development of the mean-axis reference frame for flexible aircraft," *Journal of Aircraft*, Vol. 56, No. 1, 2019, pp. 392–397.

[18] Schmidt, D. K., *Modern flight dynamics*, McGraw-Hill Higher Education, 2012.

[19] Meirovitch, L., and Tuzcu, I., "The lure of the mean axes," *Journal of Applied Mechanics*, Vol. 74, No. 3, 2007, pp. 497–504. doi:10.1115/1.2338060.

[20] Li, N., Grant, P., and Abbasi, H., "A comparison of the fixed-axes and the mean-axes modeling methods for flexible aircraft simulation," AIAA Guidance, Navigation, and Control and Co-located Conferences, American Institute of Aeronautics and Astronautics, 2010. doi:10.2514/6.2010-7605.

[21] Meirovitch, L., and Tuzcu, I., "Unified theory for the dynamics and control of maneuvering flexible aircraft," *AIAA Journal*, Vol. 42, No. 4, 2004, pp. 714–727. doi:10.2514/1.1489.

[22] D'Eleuterio, G. M. T., and Barfoot, T. D., "A discrete quasi-coordinate formulation for the dynamics of elastic bodies," *Journal of Applied Mechanics*, Vol. 74, No. 2, 2006, pp. 231–239. doi:10.1115/1.2189873.

[23] Gibson, T., Annaswamy, A., and Lavretsky, E., "Modeling for Control of Very Flexible Aircraft," American Institute of Aeronautics and Astronautics, 2011. doi:10.2514/6.2011-6202.

[24] Avanzini, G., Nicassio, F., and Scarselli, G., "Reduced-Order Short-Period Model of Flexible Aircraft," *Journal of Guidance, Control, and Dynamics*, Vol. 40, No. 8, 2017, pp. 2017–2029. doi:10.2514/1.G002387.

[25] Gonzalez, P., Starvorinus, G., Silvestre, F. J., Voß, A., Meddaikar, Y. M., and Krueger, W., "TU-Flex: A Very-Flexible Flying Demonstrator with a Generic Transport Aircraft Configuration," *AIAA SCITECH 2023 Forum*, 2023, p. 1312.

[26] Karpel, M., Shousterman, A., Maderuelo, C., and Climent, H., "Dynamic aeroservoelastic response with nonlinear structural elements," *AIAA Journal*, Vol. 53, No. 11, 2015, pp. 3233–3239.

[27] Karpel, M., "Reduced-order aeroelastic models via dynamic residualization," *Journal of Aircraft*, Vol. 27, No. 5, 1990, pp. 449–455.

[28] Theis, J., Takarics, B., Pfifer, H., Balas, G. J., and Werner, H., "Modal matching for LPV model reduction of aeroservoelastic vehicles," *AIAA Atmospheric Flight Mechanics Conference*, 2015, p. 1686.

[29] Sanghi, D., Riso, C., Cesnik, C. E. S., and Vetrano, F., "Impact of Control-Surface Flexibility on the Dynamic Response of Flexible Aircraft," *AIAA Scitech 2020 Forum*, 2020, p. 1185.

[30] Riso, C., Sanghi, D., Cesnik, C. E. S., Vetrano, F., and Teufel, P., "Parametric Roll Maneuverability Analysis of a High-Aspect-Ratio-Wing Civil Transport Aircraft," *AIAA Scitech 2020 Forum*, 2020, p. 1191.